Electronic Supplementary Material (ESI) for Journal of Materials Chemistry A.


# Supporting Information

## Optimized Nitrogen-Doped Carbon with Hierarchically Porous Structure as Highly Efficient Cathode for Na-$O_2$ Batteries

Jin-ling Ma,and Xin-bo Zhang*

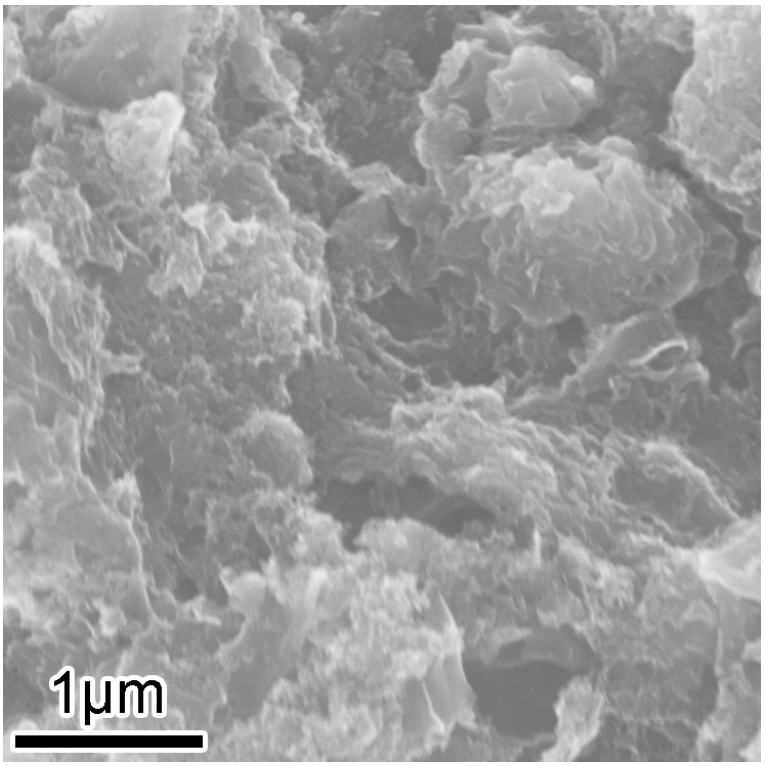


**Fig. S1** SEM image of the NC-based material.

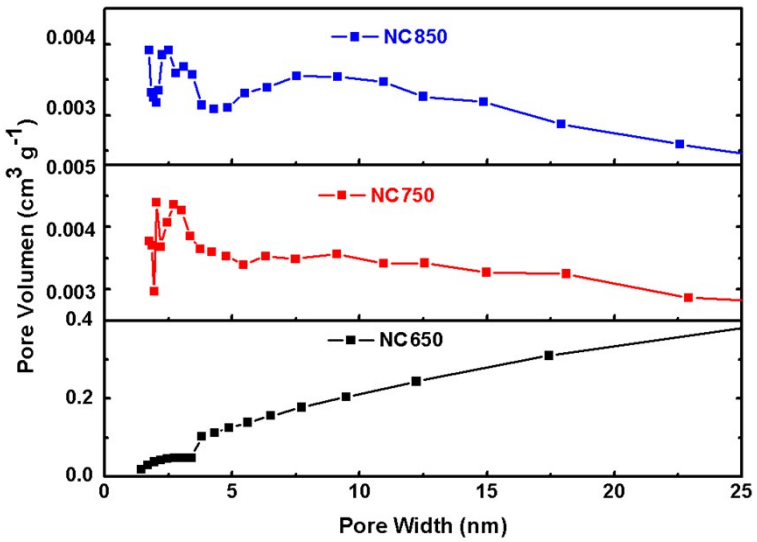


**Fig. S2** Pore size distribution curves of the NC-based materials.

**Table S1.** N content of the five samples determined by CHNS element analysis.

| Material | NC650 | NC750 | NC850 | NNC |
|---|---|---|---|---|
| N content (%) | 12.88 | 10.91 | 6.18 | 1.82 |

**Table S2.** Summary of reported electrochemical performance of Na-air/$O_2$ cells with carbon-based cathodes.

| **Cathode** | **Loading (mg)** | **Discharge current density (mA $g^{-1}$)** | **Discharge capacity (mAh $g^{-1}$)** | **Cycle life** | **Limited Capacity for Cycling (mAh $g^{-1}$)** | **Products** | **Reference** |
|---|---|---|---|---|---|---|---|
| N330 carbon | 0.25 | 75 | 2700 | 3 | 500 | $NaO_2$, $Na_2O_2$ | [S1] |
| Super P | 0.76-1.28 | 70 | 3600 | -- | -- | $Na_2O_2$, $Na_2CO_3$, $Na_2C_2O_4$ | [S2] |
| NCNTs | 0.24-0.36 | 25 | 1887 | 50 | av. 350 | $NaO_2$, $Na_2O_2$ | [S3] |
| NC750 | 0.5 | 200 | 5749 | 66 | 500 | $NaO_2$, $Na_2O_2$ | This work |

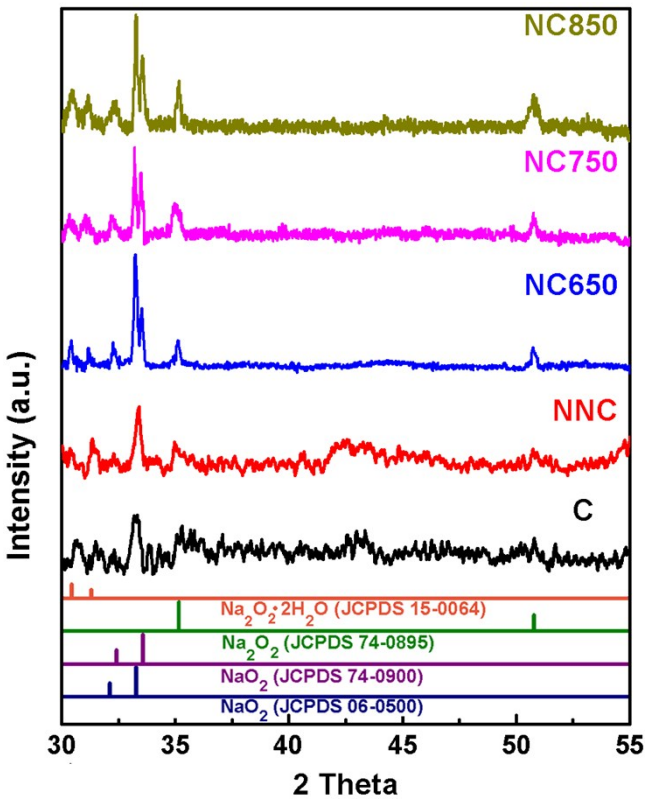


**Fig. S3** XRD patterns of the discharge products on the five cathodes.

It can be found that both sodium superoxide and peroxide appear in Na-$O_2$ cells, which is consistent with reported resutls.[S4-5] And there are two $NaO_2$ phases exist in these cathodes, possibly resulting from complicated reaction mechanism and/or the crystalline structures conversion with time.[S6] It should be noted that the intensity of $NaO_2$ is higher than that of $Na_2O_2$, indicating the preference of one-charge transfer in our system. Furthermore, $NaO_2$ and $Na_2O_2$ can easily react with $H_2O$ (from electrolyte and atmosphere) to form $Na_2O_2 \cdot 2H_2O$.

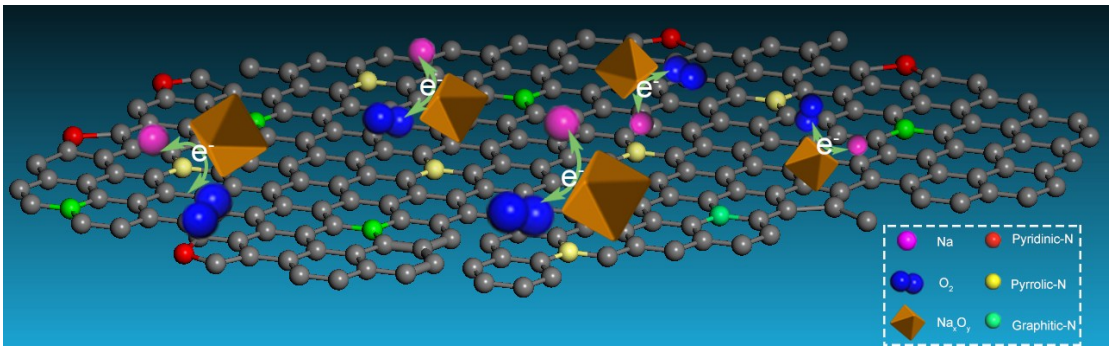


**Scheme S1.** Illustration of the mechanism for decomposition of discharge products on N-doped carbon cathodes.

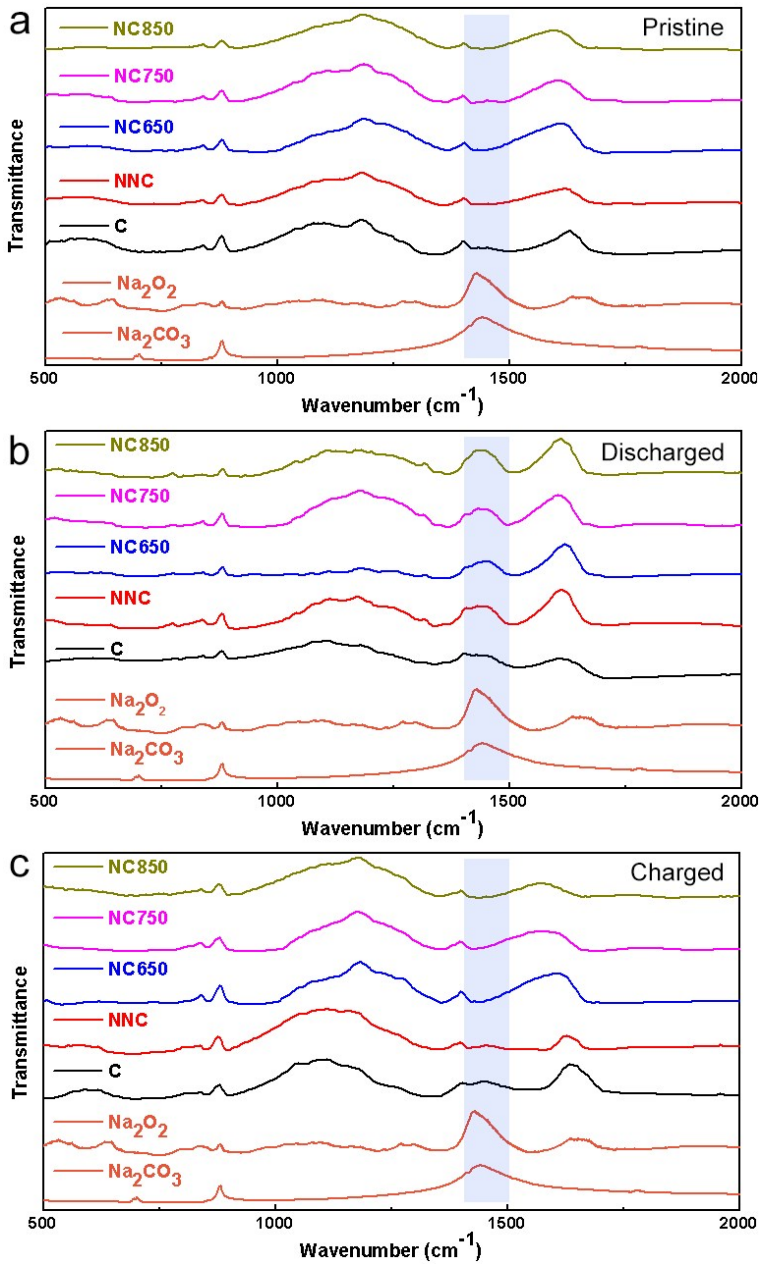


**Fig. S4** FTIR of the pristine (a), the discharged (b), and the charged (c) cathode of the C, NNC, NC650, NC750, and NC850 respectively, in Na-$O_2$ batteries.

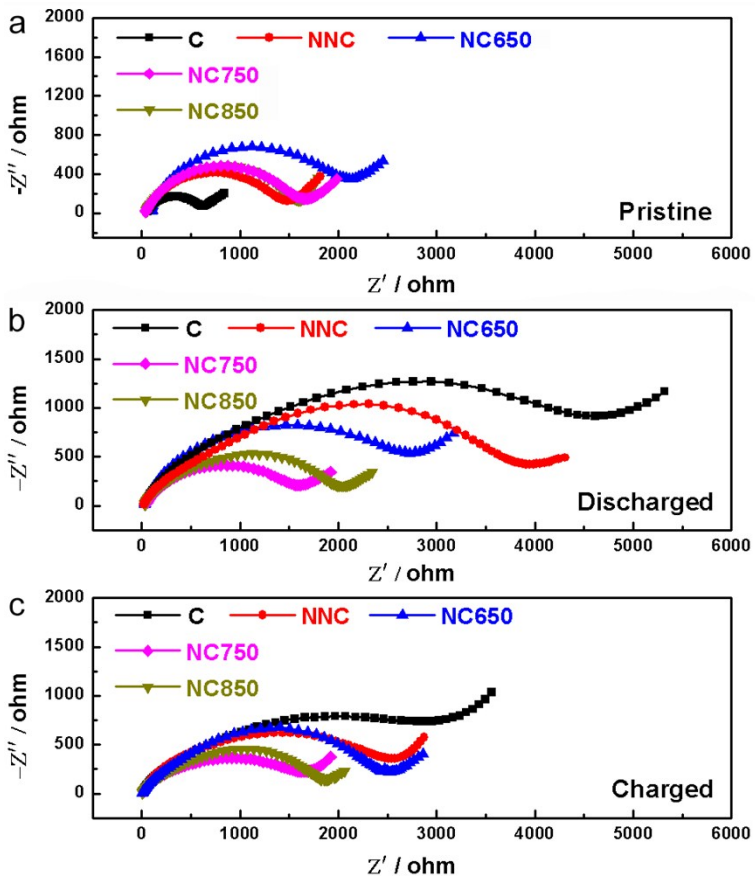


**Fig. S5** EIS for Na-$O_2$ batteries with the C, NNC, NC650, NC750, and NC850 cathodes before discharging (a), after the first discharging (b), and after the first charging (c).

**Table S3.** The electronic conductivity of the C, NNC, NC850, NC750, NC650 catalyst, respectively.

| Cathode | C | NNC | NC850 | NC750 | NC650 |
|---|---|---|---|---|---|
| Electronic conductivity (S $cm^{-1}$) | 1.58 | 1.15 | 0.97 | $1.25\times10^{-1}$ | $7.57\times10^{-2}$ |

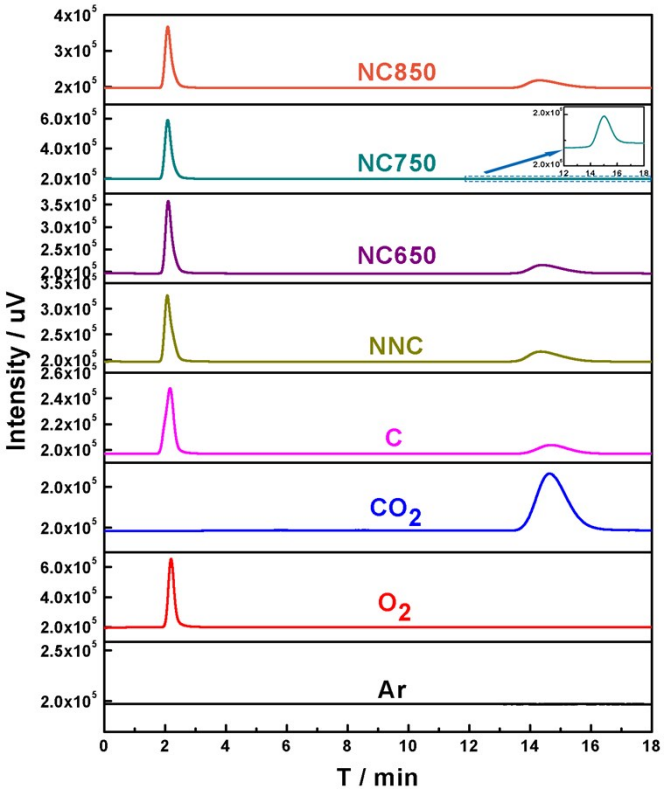


**Fig. S6.** GC resutls for $O_2$ and $CO_2$ released after charging in Na–$O_2$ cells with these cathode.

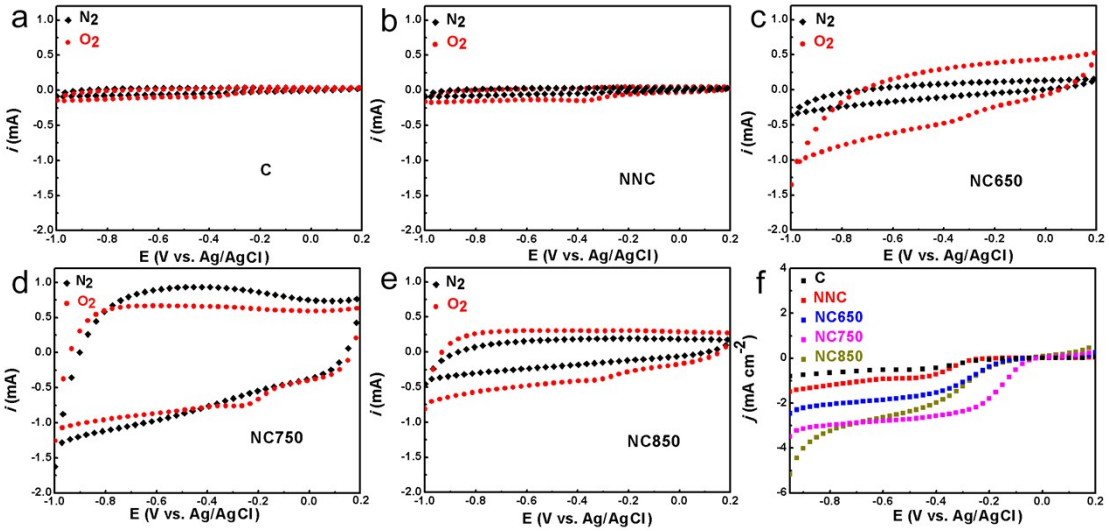


**Fig. S7** CV curves in $N_2$-saturated and $O_2$-saturated 0.1 M KOH for the C (a), NNC (b), NC650 (c), NC750 (d), NC850 (e) catalyst, and the corresponding ORR polarization curves at 1600 rpm (f).

In Fig. S7a-e, no obvious redox peak is observed for the five samples in $N_2$-saturated solution. But when the solution is saturated with $O_2$, a well-defined cathodic peak appears in these samples, confirming the electrocatalytic activity toward ORR. Note that the increase of the double-layer capacitance for as-prepared samples emerges when the soluiton is saturated with $O_2$, which is likely due to the contribution of ORR current and some surface oxidation of these samples under ORR test (-1 to 0.2 V). Typically, the incomplete carbonization of NC650 endows it with much defects (Figure 2b), making it easy be oxidized under the ORR tests and thus resulting in the increase of the capacitance. As for NC850, it exhibits relatively low ORR performance and generates much mediate oxygen-containing products which are hard to depart from the surface of the catalyts immediately during the ORR process,

accouting for the increase of the capacitance. Compared with the other samples, the more positive ORR peak potential as well as highest onset potential and largest cathodic current density achieved by NC750 suggests that optimized nitrogen content, species, and porous structure of the N-doped carbon materials play a critical role in catalysis (Fig. S7f).

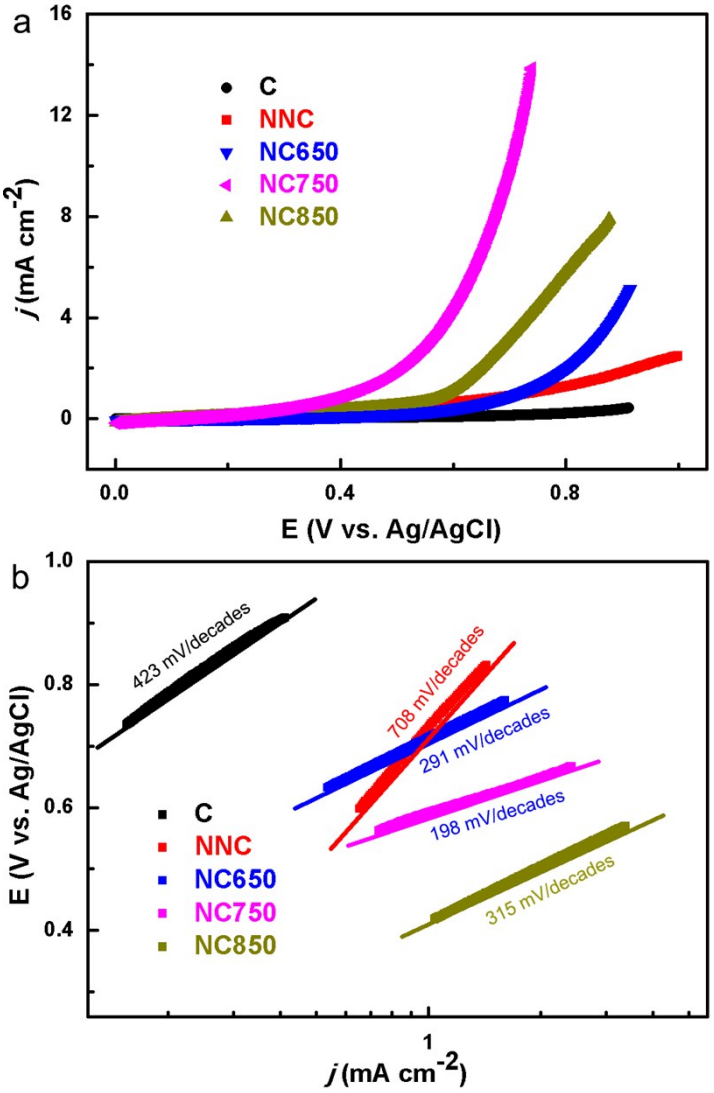


**Fig. S8** (a) ORR polarization curves for C, NNC, NC650, NC750, NC850, and (b) the accorrding Tafel plots.

**Table S4.** Comparison of ORR and OER performance.

| Materials | NC850 | NC750 | NC650 | NNC | C |
|---|---|---|---|---|---|
| Onset potetial for ORR (V vs. Ag/AgCl) | -0.15 | -0.04 | -0.16 | -0.26 | -0.29 |
| Kinetic limiting current for ORR (mA $cm^{-2}$) | 2.23 | 2.33 | 1.61 | 0.80 | 0.45 |
| Onset potetial for OER (V vs. Ag/AgCl) | 0.68 | 0.52 | 0.81 | 0.89 | 0.92 |
| Tafel slope for OER (mV/decade) | 315 | 198 | 291 | 708 | 423 |

S1 H. Yadegari, Y. Li, M. N. Banis, X. Li, B. Wang, Q. Sun, R. Li, T. K. Sham, X. Cui, X. Sun, *Energy Environ. Sci.,* 2014, **7**, 3747.

S2 S. K. Das, S. Xu, L. A. Archer, *Electro. Commun.,* 2013, **27**, 59.

S3 Q. Sun, H. Yadegari, M. N. Banis, J. Liu, B. Xiao, B. Wang, S. Lawes, X. Li, R. Li, X. Sun, *Nano Energy,* 2015, **12**, 698.

S4 S. Kang, Y. Mo, S. P. Ong, G. Ceder, *Nano Lett.,* 2014, **14**, 1016.

S5 C. L. Bender, D. Schröder, R. Pinedo, P. Adelhelm, J. Janek, *Angew. Chem., Int. Ed.,* 2016, **55**, 4640.

S6 J. Kim, H. Park, B. Lee, W. M. Seong, H. D. Lim, Y. Bae, H. Kim, W. K. Kim, K. H. Ryu, K. Kang, *Nat. Commun.,* 2016, **7**, 10670.